Acta Crystallographica Section F
Structural Biology and Crystallization Communications
ISSN 1744-3091

The high-resolution structure of the extracellular domain of human CD69 using a novel polymer

Petr Kolenko,[a]* Tereza Skálová,[a] Ondřej Vaněk,[b,c] Andrea Štěpánková,[a] Jarmila Dušková,[a] Jindřich Hašek,[a] Karel Bezouška[b,c] and Jan Dohnálek[a]

[a]Institute of Macromolecular Chemistry AS CR, v.v.i., Heyrovského nám. 2/1888, 162 06 Praha 6, Czech Republic, [b]Department of Biochemistry, Faculty of Science, Charles University, Hlavova 8, 12840 Praha 2, Czech Republic, and [c]Institute of Microbiology AS CR, v.v.i., Vídeňská 1083, 142 00 Praha 4, Czech Republic

Correspondence e-mail: kolenko@imc.cas.cz

Received 6 October 2009
Accepted 20 October 2009

PDB Reference: extracellular domain of human CD69, 3hup, r3hupsf.

The structure of the extracellular domain of human CD69 has been determined by single-crystal X-ray diffraction. The structure refined to 1.37 Å resolution provides further details of the overall structure and the asymmetric interface between the monomers in the native dimer. The protein was crystallized using di[poly(ethylene glycol)] adipate, which also served as a cryoprotectant. This is the first report of a crystal structure determined using crystals grown with this polymer.

1. Introduction

One of the first cell-surface molecules to appear following lymphocyte activation is CD69, which is expressed on a variety of haematopoietic cells, including T, B and natural killer (NK) cells, monocytes, neutrophils and platelets (Testi *et al.*, 1994). The functional effects of cross-linking cell-surface CD69 with antibodies suggest a role for CD69 as a costimulatory activation molecule, leading to proliferation, cytokine secretion, Ca^{2+} mobilization and cytotoxic responses (Testi *et al.*, 1989). The cross-linking of CD69 expressed on monocytes, neutrophils and platelets leads to nitric oxide release, degranulation and aggregation, respectively. Moreover, CD69 expression is elevated in T and NK cells infiltrating tumours (Van den Hove *et al.*, 1997). NK cells primed by incubation with tumour cells acquire the ability to lyse leukaemic cell lines and even solid tumours with the involvement of CD69 receptors, as demonstrated by the ability to inhibit such lysis using soluble recombinant extracellular domain of CD69 protein (North *et al.*, 2007).

Human CD69 is a disulfide-linked homodimer with subunits of molecular mass 28 or 32 kDa resulting from different glycosylation at two possible extracellular N-glycosylation sites (Vance *et al.*, 1997). It belongs to the type II integral membrane proteins and possesses an extracellular C-terminal protein motif related to C-type animal lectins, commonly named the C-type lectin-like domain (CTLD). The CTLD fold was first identified in a group of C-type (Ca^{2+}-dependent) animal lectins that mediate both pathogen recognition and cell–cell communication by means of protein–carbohydrate interactions (Drickamer & Taylor, 1993). CTLDs that are predicted to bind carbohydrates through coordination to a conserved Ca^{2+} ion are also known as carbohydrate-recognition domains (CRDs). However, increasing evidence shows that many of the modules that adopt the CTLD fold lack the Ca^{2+}-coordinating residues that mediate the classical C-type lectin saccharide binding, suggesting that they may serve functions other than saccharide recognition (Drickamer, 1999) or that saccharide binding takes place in a different way. The CTLD fold is widely represented among proteins that mediate the innate immune response. In particular, a conserved genomic region known as the natural killer gene cluster (NKC) encodes a group of receptors with CTLD-containing sequences, including CD69, that are involved in modulation of NK-cell activity and natural host defence (Vivier *et al.*, 2008). Despite its widespread distribution and expression, the precise function of CD69 in haematopoietic cells and its role in immune defence against tumours remains unknown and awaits the identification of its physiological ligand.

Table 1
Data-collection and refinement statistics.

Values in parentheses are for the outer resolution shell.

X-ray source, beamline	BESSY II, BL14.1
Wavelength (Å)	0.918
Resolution (Å)	30.00–1.37 (1.40–1.37)
Space group	$P6_1$
Unit-cell parameters (Å)	$a = b = 86.07$, $c = 61.98$
No. of observations	604711
No. of unique reflections	51840
Completeness (%)	94.5 (65.8)
Redundancy	7.4 (5.9)
$R_{\rm merge}$	0.054 (0.588)
$I/\sigma(I)$	34.1 (2.6)
Wilson B factor (Å^2)	16
No. of residues in ASU	239
No. of water molecules	285
Other localized ions	5 Cl^-, 1 Na^+
No. of localized non-H atoms	2389
R.m.s.d. bonds (Å)	0.01
R.m.s.d. angles (°)	1.11
Mean ADP for protein atoms (Å^2)	22
Mean ADP for solvent molecules (Å^2)	46
Mean ADP for all atoms (Å^2)	25
$R_{\rm work}$	0.133
$R_{\rm free}$	0.184
$R_{\rm all}$	0.135
No. of reflections for $R_{\rm free}$ calculation	1982 [4%]

In this study, we aimed at finding new crystallization conditions for the extracellular domain of CD69 (edCD69) that might enable the successful cocrystallization of CD69 with some of its proposed low-molecular-weight ligands. This also involved a search for new polymer-based precipitants suitable for protein crystallization. While we have not yet succeeded in cocrystallization, we have found a novel polymer suitable for crystallization of CD69 and of other proteins that allowed us to determine the crystal structure of edCD69 at the highest resolution described to date.

2. Methods

Briefly, a plasmid containing DNA coding for residues 70–199 of human CD69 was used for transformation into *Escherichia coli* BL21 (DE3) RIL. The refolded protein was further purified using an SP-Sepharose FF column (GE Healthcare Europe, Munich, Germany), a Vydac C4 reverse-phase column (Dionex, Sunnyvale, California, USA) and finally a Superdex 200 HR 10/30 column (GE Healthcare). A more detailed description of the protein production has been published elsewhere (Vaněk *et al.*, 2008). Crystals were prepared using the hanging-drop vapour-diffusion method. The protein solution consisted of 15 mg ml^{-1} edCD69 in buffer containing 100 m*M* NaCl, 10 m*M* HEPES pH 7.0, 1 m*M* NaN_3. A crystal with a longest dimension of about 560 µm crystallized from a drop containing 1 µl protein solution and 1 µl reservoir solution containing 0.1 *M* imidazole pH 6.6, 30%(*v*/*v*) di[poly(ethylene glycol)] adipate (Sigma–Aldrich, catalogue No. 494852) at a temperature of 291 K. Finally, the crystal was flash-cooled in mother liquor using liquid nitrogen prior to diffraction data collection. No additional cryoprotection was necessary.

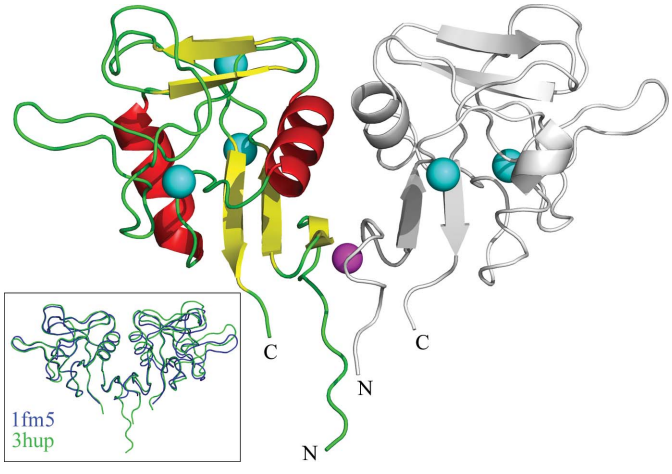

Figure 1
The structure of edCD69 represented by coloured secondary-structure elements (chain *B* in grey; sodium ion in magenta; chlorides are represented as cyan spheres). Insert: superposition of the symmetric dimer (blue, PDB code 1fm5) and the reported structure with the asymmetric interface (green, PDB code 3hup) in coil representation; the secondary-structure matching algorithm was applied to one half of the dimer.

Table 2
Characteristics of available structures of human edCD69.

$c_{\rm protein}$ is the protein concentration during crystallization.

PDB code	$c_{\rm protein}$ (mg ml^{-1})	Resolution (Å)	Space group	ASU content (construct length)	$R/R_{\rm free}$
1fm5	5	2.27	$P3_121$	Monomer (64–199)	0.24/0.30
1e8i	5	1.95	$P4_32_12$	Dimer (82–199)	0.25/0.27
3cck	5	1.80	$P6_1$	Dimer (82–199)	0.19/0.22
1e87	5	1.50	$P3_121$	Monomer (82–199)	0.23/0.25
3hup	15	1.37	$P6_1$	Dimer (70–199)	0.13/0.18

Diffraction data were collected on beamline ID14-1 at BESSY II (Berlin). To optimize the measurement for the dynamic range of the detector, two data sets were collected (90 images of low-resolution data and 110 images of high-resolution data). The data were collected at a temperature of 100 K with an oscillation angle of 1° and were processed with the *HKL* program package (Otwinowski & Minor, 1997). The crystal belonged to space group $P6_1$. Analysis of the diffraction data showed merohedral twinning of the crystal ($\alpha_{\rm twin} \simeq 12\%$). The data-processing statistics are given in Table 1.

The structure is isomorphous to a previously determined structure of human edCD69 in space group $P6_1$ (PDB code 3cck; Vaněk *et al.*, 2008). A retrospective analysis of the structure-factor amplitudes deposited with the previous structure of edCD69 in space group $P6_1$ showed that this crystal was also merohedrally twinned ($\alpha_{\rm twin} \simeq 8\%$). Our model was refined using *phenix.refine* against the original measured intensities using the built-in algebraic detwinning protocol (Adams *et al.*, 2002); manual corrections were performed with the program *Coot* (Emsley & Cowtan, 2004).

The stereochemistry of the structure was evaluated with *MolProbity* (Lovell *et al.*, 2003) and the agreement with structure factors was evaluated using *SFCHECK* (Vaguine *et al.*, 1999).

3. Results and discussion

The extracellular domain of human CD69 (edCD69) was crystallized using di[poly(ethylene glycol)] adipate. The crystals were merohedrally twinned. In comparison with previous work, the crystals grew from a higher protein concentration (see Table 2). A crystal diffracted to 1.37 Å resolution and belonged to space group $P6_1$. The structure was solved and refined at a higher resolution compared with other structures of edCD69 deposited in the PDB (Table 2). The overall structure does not differ significantly from previous structures of edCD69. Two compact domains related by a noncrystallographic twofold axis, each stabilized by three disulfides, form the noncovalent dimer, with an interface area of 850 Å^2 (Krissinel & Henrick, 2007).

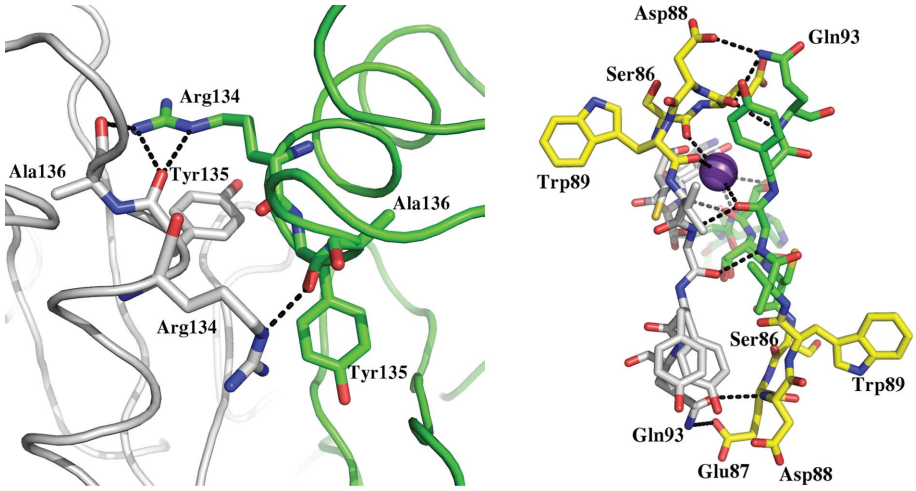

Figure 2
Interface details of the edCD69 dimer. (*a*) The amino-acid residues of the C-termini of the interface helices adopt different conformations and participate in different interactions. The Arg134 side chain involved in the π–π interaction with Tyr135 adopts a substantially different conformation in the other chain and participates in different interactions. (*b*) The N-terminal region with the sodium ion at the dimer interface. The ion-binding loop differs from the pseudosymmetric arrangement by a flipped peptide bond between Glu87 and Asp88. Carbon colour coding: green, chain *A*; grey, chain *B*; yellow, sodium-binding loop (residues Ser86–Trp89) and the pseudosymmetric chain.

One sodium ion and five chloride ions are present in the asymmetric unit (Fig. 1).

Asp79 and Val82 were the first residues to be localized in electron density for chains *A* and *B*, respectively. The N-terminal region of chain *A* participates in intermolecular interactions with a symmetry-related molecule; therefore, residues Asp79–His81 are more stabilized and interpretable in chain *A* than in chain *B*. The segment of residues Ser78–Ser80 was also observed in the first structure of edCD69 (PDB code 1fm5; Natarajan *et al.*, 2000). The structure reported here at higher resolution enables more accurate determination of this region.

The interface of the edCD69 dimer is built asymmetrically (Fig. 2). Ten residues adopt different conformations in comparison with the opposite chain to form a stabilized dimer. The most significant differences between the chains are found at the top of the helix at the interface (residues Lys133–Ala136) and in the N-terminal region (residues Asp79–Trp89). The different conformation of the helix residues was modelled as a static disorder in the structure determined by Llera *et al.* (2001; PDB code 1e87).

In the structure reported here, the N-terminal region (residues Ser86–Trp89) of chain *B* forms a loop suitable for the binding of a sodium ion with the participation of the carbonyl O atom of Gly91 in chain *A*. The main chain of residues Ser86–Trp89 in chain *A*, which has a different conformation, does not form the sodium-binding loop and a water molecule is observed in the pseudosymmetric position.

In the first crystal structure of edCD69 in space group $P3_121$ (PDB code 1fm5; Natarajan *et al.*, 2000), which has a monomer in the asymmetric unit and a precise twofold symmetry axis generating a biological unit, the dimer asymmetry was not observed. The biological significance of the symmetric *versus* asymmetric arrangement of the dimer interface remains unclear. The sodium ion is very likely to also be present in other edCD69 structures, but has never been interpreted as an ion. According to our analysis of the reported structure, the presence of the ion in one chain correlates with the overall asymmetry of the dimer interface and of the stem region.

Di[poly(ethylene glycol)] adipate is a precipitant that has potential application in other crystallization experiments. Di[poly(ethylene glycol)] adipate functions as a cryoprotectant at a concentration of 30%(*v*/*v*).

This work was supported by the European Commission (Integrated Project SPINE2-COMPLEXES, contract No. 031220), by the Grant Agency of the Academy of Sciences of the Czech Republic (project IAA500500701) and by the Grant Agency of the Czech Republic (projects 305/07/1073 and 303/09/0477). We acknowledge the use of beamline BL14.1 at the synchrotron-radiation source BESSY II, Helmholtz-Zentrum Berlin, assistance by U. Müller and funding of user access by the EC under ELISA grant No. 226716.

References

Adams, P. D., Grosse-Kunstleve, R. W., Hung, L.-W., Ioerger, T. R., McCoy, A. J., Moriarty, N. W., Read, R. J., Sacchettini, J. C., Sauter, N. K. & Terwilliger, T. C. (2002). *Acta Cryst.* D**58**, 1948–1954.
Drickamer, K. (1999). *Curr. Opin. Struct. Biol.* **9**, 585–590.
Drickamer, K. & Taylor, M. E. (1993). *Annu. Rev. Cell Biol.* **9**, 237–264.
Emsley, P. & Cowtan, K. (2004). *Acta Cryst.* D**60**, 2126–2132.
Krissinel, E. & Henrick, K. (2007). *J. Mol. Biol.* **372**, 774–797.
Llera, A. S., Viedma, F., Sanchez-Madrid, F. & Tormo, J. (2001). *J. Biol. Chem.* **276**, 7312–7319.
Lovell, S. C., Davis, I. W., Arendall, W. B. III, de Bakker, P. I., Word, J. M., Prisant, M. G., Richardson, J. S. & Richardson, D. C. (2003). *Proteins*, **50**, 437–450.
Natarajan, K., Sawicki, M. W., Margulies, D. H. & Mariuzza, R. A. (2000). *Biochemistry*, **39**, 14779–14786.
North, J., Bakhsh, I., Marden, C., Pittman, H., Addison, E., Navarrete, C., Anderson, R. & Lowdell, M. W. (2007). *J. Immunol.* **178**, 85–94.
Otwinowski, Z. & Minor, W. (1997). *Methods Enzymol.* **276**, 307–326.
Testi, R., D'Ambrosio, D., De Maria, R. & Santoni, A. (1994). *Immunol. Today*, **15**, 479–483.
Testi, R., Phillips, J. H. & Larnier, L. L. (1989). *J. Immunol.* **143**, 1123–1128.
Vaguine, A. A., Richelle, J. & Wodak, S. J. (1999). *Acta Cryst.* D**55**, 191–205.
Vance, B. A., Wu, W., Ribaudo, R. K., Segal, D. M. & Kearse, K. P. (1997). *J. Biol. Chem.* **272**, 23117–23122.
Van den Hove, L. E., Van Gool, S. W., Van Poppel, H., Baert, L., Coorevits, L., Van Damme, B. & Ceuppens, J. L. (1997). *Clin. Exp. Immunol.* **109**, 501–509.
Vaněk, O. *et al.* (2008). *FEBS J.* **275**, 5589–5606.
Vivier, E., Tomasello, E., Baratin, M., Walzer, T. & Ugolini, S. (2008). *Nature Immunol.* **9**, 503–510.